Characterization of a Folding Intermediate of Human Carbonic Anhydrase II: Probing Local Mobility by Electron Paramagnetic Resonance

Mikael Lindgren,* Magdalena Svensson,‡ Per-Ola Freskgård,‡ Uno Carlsson,‡ Per Jonasson,§ Lars-Göran Mårtensson,§ and Bengt-Harald Jonsson§

Departments of *Chemical Physics and ‡Chemistry, Linköping University, S-581 83 Linköping, and §Department of Biochemistry, Umeå University, S-90187 Umeå, Sweden

ABSTRACT The spin-labeling method was used to investigate human carbonic anhydrase, HCA II, undergoing unfolding induced by guanidine-HCl (Gu-HCl). The spin-probe, *N*-(2,2,5,5-tetramethyl-1-yloxypyrrolidinyl-3-yl)iodoacetamide, was attached covalently to the single cysteine (position 206) in the enzyme. The electron paramagnetic resonance spectrum of the folded structure showed the characteristic slow motional spectra. When the concentration of the denaturing agent, Gu-HCl, was gradually increased, new spectral components with narrower lines evolved to give complex electron paramagnetic resonance spectra, apparently containing superimposed contributions from several components of different mobility. By a differentiation technique, it was possible to follow the relative increase of the narrow components as a function of Gu-HCl concentration. The amplitude of difference spectra versus Gu-HCl concentration showed two distinct maxima, indicating the existence of a folding intermediate state/structure. The results were found to agree with optical absorption data, which showed similar transitions at the same Gu-HCl concentrations. From line-shape simulations assuming a Brownian diffusion model, the rotational diffusion constants for the spin-label in the folded, folding intermediate, and unfolded structures were determined. The relative abundances of the three conformations in the region 0–4 M Gu-HCl were obtained by least squares fitting of the simulated spectra to the experimental ones. The folding intermediate was found to have a maximum population of 39 ± 4% at ~0.7 M Gu-HCl.

INTRODUCTION

Learning more about the details of the folding and unfolding mechanisms of globular proteins has become a central issue in the development of protein engineering (Endo, 1991; Pain, 1987). This quest for knowledge has encouraged biochemists and biophysicists to explore the application of modern spectroscopic methods in determining protein structure during unfolding and refolding pathways. For example, nuclear magnetic resonance has been used to characterize intermediate structures of various proteins. In these studies, structural information about folding intermediates is obtained indirectly by using the hydrogen/deuterium exchange method (Englander, 1993). Electron paramagnetic resonance (EPR) in combination with spin-probing methods has attracted increased attention in studies of biological macromolecular systems (Millhauser, 1992). An analysis of the spectra can provide a detailed picture of the interaction with neighboring side chains and solvent molecules. This approach has recently been used to study specific regions of colicin E1 and also the insertion into a membrane (Todd et al., 1989; Shin et al., 1993) and specific interaction in bacteriorhodopsin (Altenbach et al., 1989) as well as side chain mobility of the folded and the intermediate molten globule of β-lactamase (Calciano et al., 1993).

A covalently bonded spin-label in carbonic anhydrase (CA) II, (Carlsson et al., 1975) or mutants thereof (Lindgren et al., 1993) has been shown to give direct structural and dynamical information of the conformational state. Optical measurements and chemical labeling studies (Henkens et al., 1982; Mårtensson et al., 1992, 1993) have indicated the existence of folding intermediates observed at equilibrium at moderate concentrations of guanidine-HCl (Gu-HCl) of bovine and human carbonic anhydrase and spin-labeled mutants thereof. EPR studies of spin-labeled mutants also indicated the presence of folding intermediates (Lindgren et al., 1993).

Cloned human carbonic anhydrase, HCA II, and mutants thereof unfold with two distinct transitions when the concentration of denaturant, Gu-HCl, is raised from 0 to 5 M, indicating the existence of a folding intermediate (Mårtensson et al., 1992, 1993). The transitions were established by recording the change in absorbance at 292 nm, which depends on exposure of buried tryptophans to solvent during the unfolding process. The present report provides EPR evidence of at least one folding intermediate of HCA II spin-labeled at the cysteine in its normal position (206). This single cysteine in the protein is buried in the native conformation and is located close to the surface in an extensive twisted β structure passing through the molecule (Eriksson et al., 1988). Because of the burial of the cysteine it was spin-labeled in the denatured state followed by renaturation (Carlsson et al., 1975). Moreover, we show a feasible way of detecting and identifying the spin-labeled folding intermediate structures by using a difference spectra technique, which essentially gives the EPR spectra differ-

Received for publication 25 April 1994 and in final form 13 April 1995.

Address reprint requests to Dr. Mikael Lindgren, IFM-Chemical Physics, IFM-FOA, Linköping University, S-58183 Linköping, Sweden. Tel.: 011-46-13-282485; Fax: 011-46-13-142337; E-mail: mli@ifm.liu.se.

0006-3495/95/07/202/12 $2.00

entiated with respect to the concentration of the denaturing agent, Gu-HCl. With this simple technique, it is easy to follow the relative growth of new components with different line-width parameters in otherwise rather complex spectra composed of several superimposed components in an equilibrium, or the changes of the dynamical characteristics of one component, during the change of an experimental parameter. Adopting this method, we also show how the determination of rotational diffusion constants of intermediate structures/states can be considerably simplified. Finally, the simulations corresponding to the native, unfolded and an intermediate state are used to fit experimental spectra by the methods of linear least squares, and we obtain information on the relative abundances of the local conformations as a function of Gu-HCl concentration.

The dynamic state of the spin-probe at its position in the globular structure is a distinct measure of the local structure. In forthcoming studies, the method will be further used systematically to examine mutants of HCA II spin-labeled in various positions. Our preliminary studies (Lindgren et al., 1993) indicated large differences in spin-probe mobility for the folded, folding intermediate, and unfolded structures, depending on the position of the attached spin-probe.

MATERIALS AND METHODS

Sample preparation

The expression plasmid pACA (Nair et al., 1991), transformed into *Escherichia coli* strain BL21/DE3, was used for production of HCA II. The enzyme was purified by affinity chromatography (Khalifah et al., 1977) and the purity was verified by sodium dodecyl sulfate polyacrylamide gel electrophoresis. A spin-probe, *N*-(2,2,5,5-tetramethyl-1-yloxypyrrolidinyl-3-yl)iodoacetamide (Sigma Chemical Co., St. Louis, MO), was used to label the single SH moiety at position 206. The enzyme (34 μM) was allowed to react with the spin-probe (648 μM) under denaturing conditions (5.0 M Gu-HCl (Pierce, Rockford, IL) in 0.1 M Tris-H_2SO_4 (Trizma base, Sigma), pH 7.5, at 23°C for 20 h. The labeled enzyme was then reactivated by diluting to a final concentration of 0.85 μM and a Gu-HCl concentration of 0.3 M. The reactivation was allowed to proceed for 90 min. The active enzyme molecules were purified by affinity chromatography (Khalifah et al., 1977), and excesses of reagents were thereby concomitantly removed. The labeled carbonic anhydrase was then dialyzed toward 1 mM Tris-H_2SO_4, pH 7.5. After dialysis, the enzyme was concentrated to a suitable concentration before EPR and UV measurements.

UV measurements

The enzyme (8.5 μM) was first incubated in various concentrations (0–8 M) of Gu-HCl buffered with 0.1 M Tris-H_2SO_4, pH 7.5, at 23°C for 24 h. Denaturation was then monitored by measuring A_{292} as a function of Gu-HCl concentration. To compensate for variation in enzyme concentration, the A_{292}/A_{260} ratio was determined, as A_{260} has been shown to be unaffected by complete denaturation (Edsall et al., 1966).

EPR measurements

With enzyme samples prepared in the same manner as described above, EPR measurements were carried out on a Bruker EPR spectrometer that consisted of a combination of the ER 200 and ESP 300 systems. An ER4103TM cavity connected to the 200-mW microwave bridge was used in all measurements. The enzyme samples (8.5 μM) were introduced in the large standard flat cell for aqueous samples. When recording the EPR spectra, care was taken to avoid line-shape distortions that could arise from experimental conditions such as microwave saturation and overmodulation. The modulation amplitude was set lower than one-half of the line-width of the $m_I = 0$ nitrogen hyperfine transition, typically 0.02 mT (fast motion) – 0.09 mT (slow motion), at typically 1–4 mW microwave power. Samples at selected concentrations, typically at 0, 1, and 4 M Gu-HCl of spin-labeled HCA II and several mutants thereof (Lindgren et al., 1993) were used to examine the influence of microwave power on the EPR line-shape. Generally, no such distortions could be observed down to approximately 13 dB attenuation. During the recording of an experimental series as discussed herein (~20 samples), the microwave power was kept at lower values to minimize eventual undesired effects at other Gu-HCl concentrations. All experiments were carried out at room temperature (19 ± 1°C).

EPR line-shape simulations

Programs used were developed by Freed and co-workers (Schneider and Freed, 1989) to account for slow motional diffusion. The programs were modified to allow simple input/output, spectrum integration, addition/subtraction, etc. Arrays and matrices were enlarged and recompiled by using the Fortran Powerstation Program (Microsoft) under Windows. Most simulations were carried out with an MC66 486 Dell personal computer or equivalent.

The EPR parameters of the spin-label in the rigid state were refined from the ones used in our previous study (Lindgren et al., 1993), which were obtained by recording the spectrum of a frozen water solution of the spin probe. (The refined parameters were obtained by simulating the EPR spectrum associated with the spin-labeled W97C/C206S mutant in a new series of samples, using the same (new) experimental setup as the one used herein, which resulted in a much better S/N ratio. The EPR spectrum associated with this spin-labeled mutant gives a pure one-component spectrum with the rotational diffusion characteristics associated with the essentially isotropic motion of the whole protein, $\tau_R = 9.5$ ns.) The following parameters were used throughout the study: $g_x = 2.0054$, $g_y = 2.0088$, $g_z = 2.0020$, $A_x = 0.56$ mT, $A_y = 0.665$ mT, $A_z = 3.55$ mT. Typical truncation values L^e_{max}, L^o_{max} and K_{max} were 26, 25, and 24, respectively.

To account for the unresolved hyperfine splitting to hydrogens within the spin-probe, a subroutine was added, which allowed convolution of the final spectrum obtained from the TDLL subroutine (Schneider and Freed, 1989) with a Gaussian line-shape function to yield an arbitrary (selected) peak-to-peak line-width of the $m_I = 0$ transition. This was essentially the same subroutine as used previously in line-shape simulations adopting site-exchange models for anisotropic systems (Benetis et al., 1990). In this manner, the intrinsic (T_2 related) broadening parameter (Lorentzian) could be decreased at the expense of Gaussian broadening. This resulted in much better line-shape, particularly at higher Gu-HCl concentrations, because both the amplitude and widths of the $m_I = -1$, 0, and +1 transitions of the more rapidly diffusing species become more sensitive to the T_2 parameter. Each spectrum took ~10–20 s to calculate.

Fittings to experimental spectra with a linear combination of three simulated spectra were achieved by developing a least squares fitting program following the methods and subroutines (after appropriate modifications) as outlined in Numerical Recipes (Press et al., 1989) with solution of general least squares by use of singular value decomposition. The standard deviation of the fitted parameters was taken as the square root of the variances. The measurement error for each sample point (field) was calculated as the root square mean of the difference between the fitted and experimental spectra.

RESULTS AND DISCUSSION

EPR spectra at various concentrations of Gu-HCl

When the concentration of Gu-HCl is gradually increased, there is a dramatic change in the EPR line-shape. The spectra of spin-labeled HCA II at selected Gu-HCl concentrations in the range 0–4.0 M are shown in Figs. 1 and 7 (dotted curves are simulations to be discussed in sections below). At the lowest Gu-HCl concentration, a spectrum characteristic of a spin-probe in slow motion is obtained. The gradual increase in Gu-HCl concentration is followed by the appearance of new narrower peaks with the characteristic three-line hyperfine pattern of a rapidly tumbling spin-probe. At intermediate Gu-HCl concentrations the spectra appear as complex superpositions of components of different mobility.

Optical absorption

The occurrence of two transitions in equilibrium denaturation curves for HCA II as monitored by the change of absorbance at 292 nm has been suggested to imply the existence of a folding intermediate (Mårtensson et. al., 1993). The change in absorbance at 292 nm is presented in Fig. 2 as the ratio A_{292}/A_{260}, where A_{260} serves as an internal standard for protein concentration (Mårtensson et al., 1992, 1993). The loss of enzymatic activity has been shown to be related to the first of the two distinct transitions. As there are 7 tryptophan residues in HCA II, the parameter given by the A_{292}/A_{260} ratio reflects a global conformational change of the three-dimensional structure.

EPR spectra differentiation

By collecting EPR spectra of the spin-labeled protein at various concentrations of Gu-HCl we obtained a wealth of experimental data. In the intermediate Gu-HCl concentration range the individual EPR signals associated with the spin-probe are complex and differ slightly. The analysis is therefore ambiguous, as it is difficult to distinguish between the spectral changes caused by changes of dynamic parameters, such as rotational diffusion, and the changes originating from the superposition spectra of different components (having different but similar dynamic parameters) governed by an equilibrium. Moreover, as, throughout the entire Gu-HCl concentration range, we are dealing with species of identical chemical composition, i.e., that differ solely in regard to conformation, it cannot be ruled out that spectral changes to some extent originate from a rate of interchange between the different conformations that are Gu-HCl concentration dependent. If this exchange occurs on a time-scale comparable with the intrinsic diffusion constants of the spin-probe, it must also be taken into account when analyzing the EPR spectra.

Having pointed out the complexity of the problem, we will now examine the simpler aspects of the EPR spectra.

Assuming that the series of spectra represents an equilibrium between three components, as indicated by the optical absorption data presented in Fig. 2 (see also Mårtensson et al., 1992, 1993), and that the interchange between the three conformationally different states takes place at a slow rate, the approximation can be made that a small change in Gu-HCl concentration will not cause a substantial change of the dynamic parameters of each component. (Each state is independent on the time-scale of the hyperfine splitting anisotropy, which can be averaged by site-exchange between the three states.) Thus, difference spectra individually obtained by subtracting the EPR spectrum of a lower Gu-HCl concentration from the spectrum of the next higher concentration will reveal the relative increase of a component with positive phase and a decrease of a component with negative phase. If the spectra have been recorded with different spectrometer settings, it is, of course, necessary to first normalize properly before subtraction.

To clarify the subtraction procedure, normal and difference spectra at 1.7/1.5 M Gu-HCl are shown in Fig. 3. This figure also shows the integrated (absorption) spectra, which are more sensitive to present the broader components in superimposed spectra. In the first-derivative spectrum, traditionally monitored in EPR, contributions from sharp-line components dominate in amplitude. In the absorption spectrum a broader component is recognized. The difference absorption spectrum clearly shows both the broad component with a negative phase and the narrow component with a positive phase, which means that the narrow component is increasing whereas the broad component is decreasing in this Gu-HCl concentration range. In ordinary spectra (absorption as well as in first-derivative mode) such small changes are difficult to quantify from a visual inspection, unless they are quite large. (The general case is difficult to describe more quantitatively as it depends strongly on both the relative line-widths and the abundances of the superimposed components.) Thus, a series of single spectra cannot provide the needed quantitative information about spectral changes unless extremely well fitting simulations of superimposed signals are made for each spectrum and relative abundances are subsequently extracted from the simulations. However, this procedure is applicable only if the detailed EPR dynamic parameters of each contributing component are known in advance. When two different components are present these parameters can simply be determined at the extreme conditions where one component is dominating over the other, but it becomes increasingly cumbersome when more components are participating in the equilibrium, which might be expected in our case.

Proceeding now with the analysis, selected difference spectra obtained for various concentrations of Gu-HCl are shown in Fig. 4. The spectral changes are divided into two Gu-HCl ranges, Fig. 4, *a-c*, and Fig. 4, *d-f*, in which the difference spectra are of comparable amplitude. The growth of a distinct, narrow component is clearly detectable at higher Gu-HCl concentrations with a maximum at ~2 M, and a slightly broader component appears at lower Gu-HCl

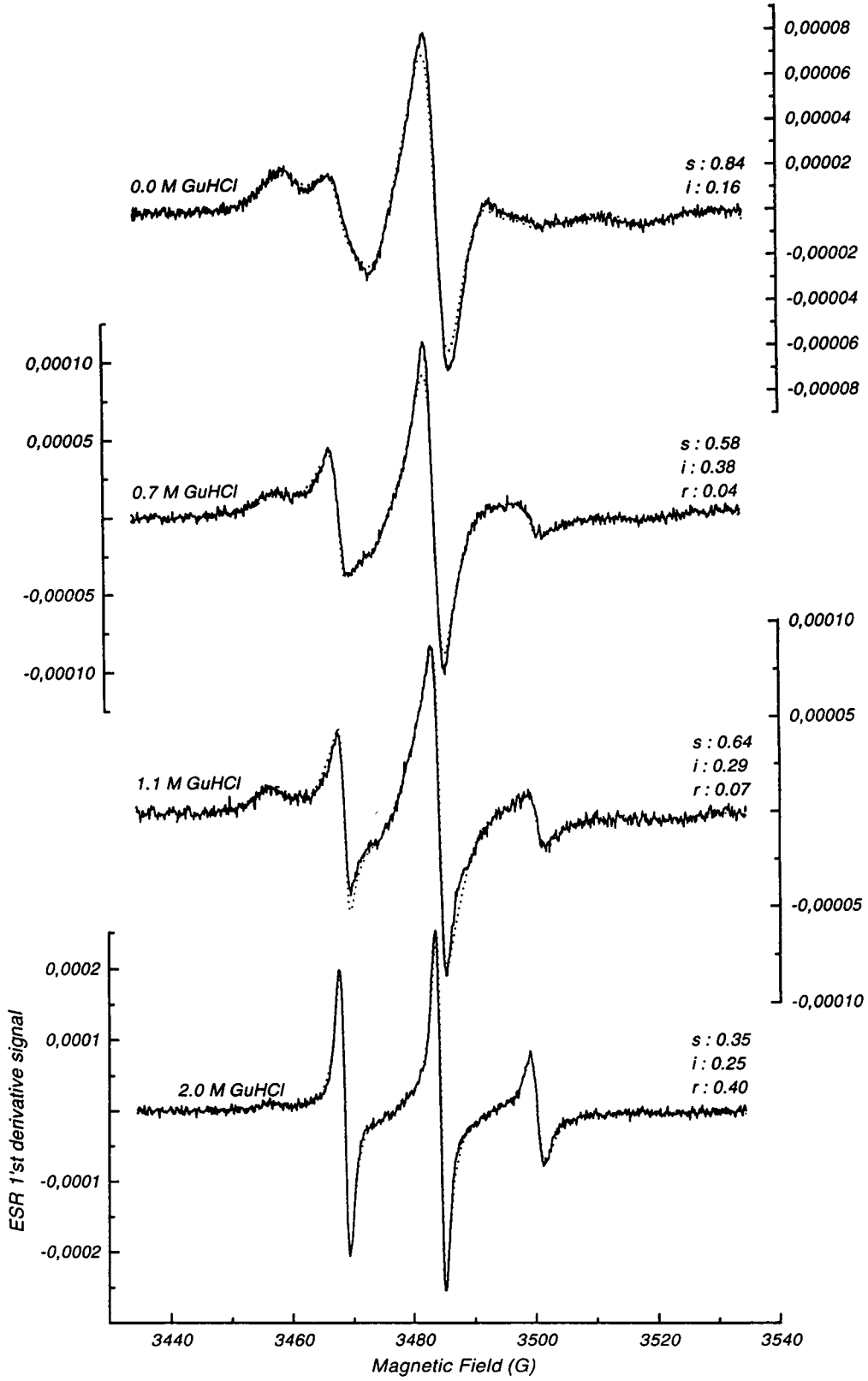

FIGURE 1 EPR spectra of cloned HCA II spin-labeled at the cysteine in position 206 recorded at selected denaturing agent (Gu-HCl) concentrations. The dashed curves are simulations produced as described in the text. The individual weights of the slow (s), intermediate (*i*), and rapid (*r*) component is given at each spectrum. All spectra are normalized and the scale beside each spectrum thus allows comparison of the amplitude at different Gu-HCl concentrations. (10 G = 1 mT.)

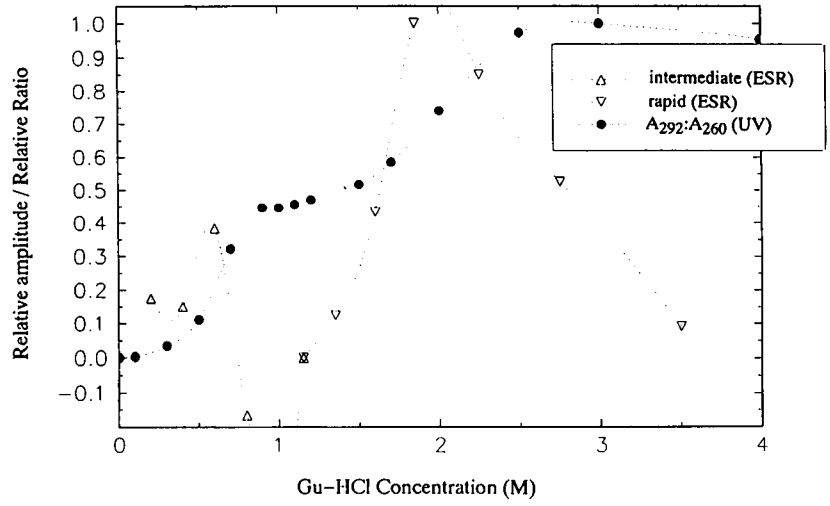

FIGURE 2 ●, The fractional change of the ratio of the absorption at 292 and 260 nm of cloned HCA II spin-labeled at the cysteine in position 206 plotted versus Gu-HCl concentration. The fractional change reflects the degree of exposure of tryptophans to solvent during the unfolding process. △ and ▽, The relative amplitude of the narrow component of EPR difference spectra obtained as described in the text. Lines connecting the points are drawn solely to guide the eye.

concentrations, with a maximum at ~0.7 M. We conclude that the former represents the spin-probe in a mobile and essentially unstructured environment, as essentially the same spectrum is obtained at higher Gu-HCl concentrations, when the contributions from the folding intermediate and the folded structure are negligible. The maximum obtained at ~0.7 M seems to represent the spin-probe in a state of intermediate mobility, as judged from its lineshape compared with those of the folded and unfolded conformations.

To ensure that the spectra differentiation procedure reflects the changes of the spin-labeled protein structure we must show that other solvent effects on the spin-probe/

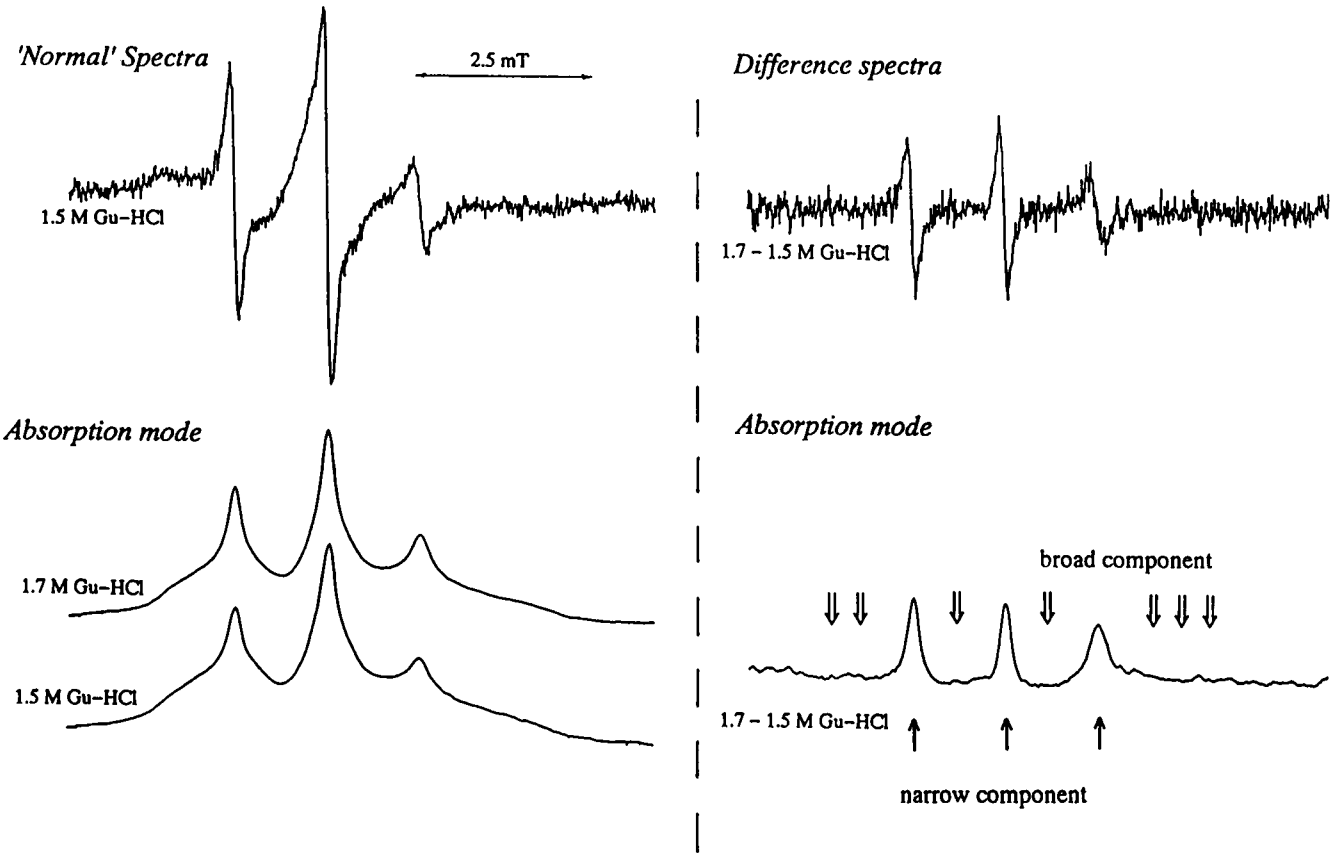

FIGURE 3 Normal and difference EPR spectra for first derivative and absorption of cloned HCA II spin-labeled at the cysteine in position 206. Normal spectra: [Gu-HCl] = 1.7 M and 1.5 M (first-derivative spectra shown only for 1.5 M). Difference spectra: ([Gu-HCl] = 1.7) − ([Gu-HCl] = 1.5). Absorption mode spectra for 1.5 M and 1.7 M are plotted to have the same amplitude of the central peak. All other spectra are plotted with arbitrary amplitude scale. 10 G = 1 mT.

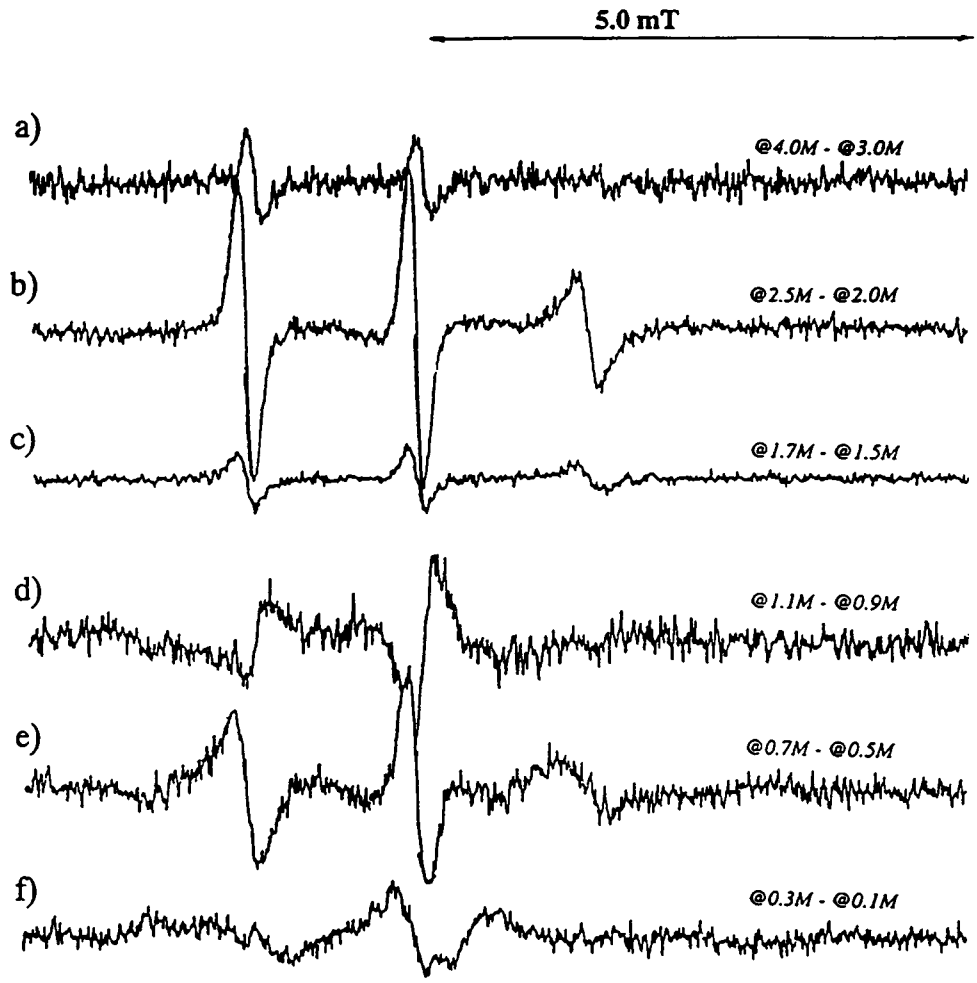

FIGURE 4 Difference EPR spectra of cloned HCA II spin-labeled at the cysteine in position 206 at selected denaturing agent (Gu-HCl) concentrations (range 0.0–3.5 M). [Gu-HCl] for difference spectrum calculation is given for each spectrum. Note that spectra *a-c* and *d-f* are plotted with different amplitude scales. 10G = 1 mT.

protein in the examined range of Gu-HCl concentrations can be excluded. (We are indebted to one of the referees who encouraged us to elaborate on these matters.) To make this appropriately it is necessary to attach the spin-probe onto the main chain of a polymer with similar composition, molecular weight, and solvent interaction with Gu-HCl/water as HCA II; a test sample is not particularly simple to find apart from spin-labeled polypeptides. (A bare molecular spin-label tumbles at a rate several orders of magnitude faster than the same spin-probe attached to a macromolecule, and the examination of the concentration dependence on the EPR line-shape could at worst give misleading results.) Certain double mutants of HCA II, W16C/C206S and F176C/C206S (W, tryptophan; C, cysteine; S, serine; F, phenylalanine), which were labeled with the same spin-probe, can in this regard serve as the desired control (for experimental details and further discussions, see Lindgren et al., 1993).

Spin-labeled W16C/C206S has the probe near a terminal region (position 16) that is remote from the core of the native protein structure. With the spin-probe in this peripheral region of the native conformation we showed previously that the associated EPR line-shape was a typical isotropic ^{14}N hyperfine triplet with different apparent amplitudes of the $m_I = -1$, 0, and +1 transitions, as is well known for spin-probes attached to polymers and other macromolecules. This line-shape was different from mutants labeled in more central regions of the native structure, which showed the characteristic slow-motional spectra, just as the case of HCA II discussed herein. The EPR signal of the spin-labeled W16C/C206S mutant showed no essential line-shape changes within the examined Gu-HCl concentration range (0–8 M), and a closer examination of these data can give a hint of the solvent/viscosity effect on the spin-label system. In Fig. 5 the amplitudes of the high and low field lines relative to the center line of the ^{14}N hyperfine triplet are plotted versus Gu-HCl concentration. The relative amplitudes (or relative line-widths) of the hyperfine lines can be used to estimate the rotational correlation times of the spin-probe (Poole and Farach, 1986). As shown in the plot, there are no essential changes between 0.5 and 4 M Gu-HCl, and in the same range of concentration the line-width of the central line is constant, 0.185 ± 0.005 mT. This ensures that difference spectra similar to those of the spin-labeled HCA II as presented in Figs. 3 and 4, are not expected. The results of F176C/C206S above ~2.0 M Gu-HCl are similar to those of W16C/C206S and have been included in Fig. 5. As indicated in the plot, minor changes

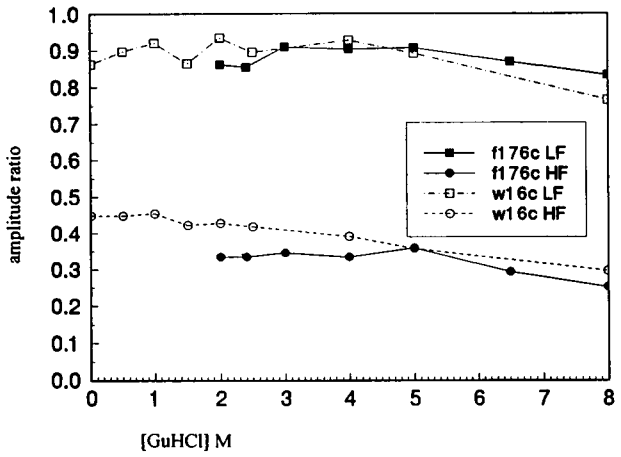

FIGURE 5 Amplitude of high (□ and ■) and low (○ and ●) field ^{14}N hyperfine lines relative to the center peak of two spin-labeled mutants: W16C/C206S (□ and ○) and F176C/C206S (■ and ●).

occur above ~5 M for both spin-labeled mutants, which probably can be related to a solvent effect. The control experiment of a sole spin-label gave essentially identical EPR spectra at 0 and 5 M Gu-HCl concentration.

Conclusively, the dramatic EPR line-shape changes observed for the spin-labeled HCA II in the Gu-HCl concentration range 0–4 M can certainly be attributed to changes of the protein conformation, and by inference, so also do the difference spectra obtained in the same Gu-HCl concentration range.

The relative amplitude of the dominating narrow peak in the difference spectra (as in Fig. 4) is plotted together with the optical absorption data versus Gu-HCl concentration in Fig. 2. (The difference spectra were calculated after normalization of all experimental spectra. The amplitude scale of each spectrum was thereafter divided with the associated step in Gu-HCl concentration. This procedure makes it possible to use experimental spectra obtained at arbitrary Gu-HCl concentrations and to present the data in a reproducible manner.) Notably, the regions of large slope of the optical absorption data occur together with maxima of the difference spectra amplitudes. This suggests that the changes shown by the optical absorption data describe the same process as revealed from the EPR spectra difference procedure. (To obtain a high resolution in Gu-HCl concentration it is of course necessary to make the step much smaller than the range over which the changes occur. However, if the steps are made too small, information is lost because of a resulting poor signal-to-noise ratio.) The shift in absorption peak monitored by the optical absorption data reflects the structural environment in terms of polarity (apolar versus polar) rather than the dynamic properties of the spin-probe. (The time-scale of an optical absorption process is short and the absorption maximum is not sensitive to diffusional motion in the range 10^7-10^9 s^{-1}, which is the case for the protein in our study.) The changes in the EPR spectra are therefore concluded to be dominated by the changes in relative abundances of the structurally and dynamically unique conformations. Thus, two peaks in the difference amplitude versus Gu-HCl concentration are in agreement with our assumption of a three-phase equilibrium for the conformational structures of the protein as it implies that two new states of rotational diffusion (associated with more narrow line-widths) are becoming populated during the increase of the Gu-HCl concentration from ~0.5 M to ~3 M. Note also that the difference spectra at 1.1 M Gu-HCl shows the intermediate state with a negative phase, implying that this state has started to decrease in abundance at this Gu-HCl concentration.

It should also be pointed out here that the clear appearance of two distinct peaks when plotting the amplitudes of the difference spectra depends on the fact that all three states are associated with different rotational mobilities of the spin-probe. If the local position of the spin-probe of the intermediate conformation gives rise to an EPR line-shape very similar to the line-shape of the spin-probe in the native or unfolded forms, only one distinct maximum is expected. We have found such cases during a systematic study of mutants having the spin-label at various positions of the protein in the native state. The results of these studies will appear elsewhere (Svensson et al., 1995).

To summarize this section, we have obtained clear EPR spectra for all three components participating in the equilibrium at the expense of having the spectra associated with medium mobility slightly distorted owing to the appearance of a broader component with a negative phase. In any case, as indicated above, the narrower component dominates in regard to amplitude, and the difference spectrum will greatly aid in the simulation of composed superpositions.

Simulations of superimposed spectra

Using simulations associated with the three spectral components obtained as described above, folded, intermediate, and unfolded, we can qualitatively explain the spectra in the Gu-HCl concentration range, in which the drastic changes occur, i.e., 0–4 M. Employing the program by Freed and co-workers (Schneider and Freed, 1989) and assuming Brownian diffusion, the spectra shown in Fig. 6 were used in simulations of superpositions (parameters are given in the figure legend).

In the simulation of the slow component, the main experimental spectral parameter used to obtain the simulated spectrum was the extrema separation (2^*A_z), which is clearly recognizable in all spectra at lower Gu-HCl concentrations. The line-width was obtained by carefully reproducing the line-shapes of the low-field and high-field transitions. Once the diffusion parameters had been used to set the extrema separation, the line-width parameters (intrinsic Lorentzian and Gaussian) were easily obtained. By trying various kind of parameters for both isotropic and anisotropic (axial) rotational diffusion it was established that the experimental spectrum obtained at 0 M Gu-HCl must contain at least two separate contributions. Furthermore, as

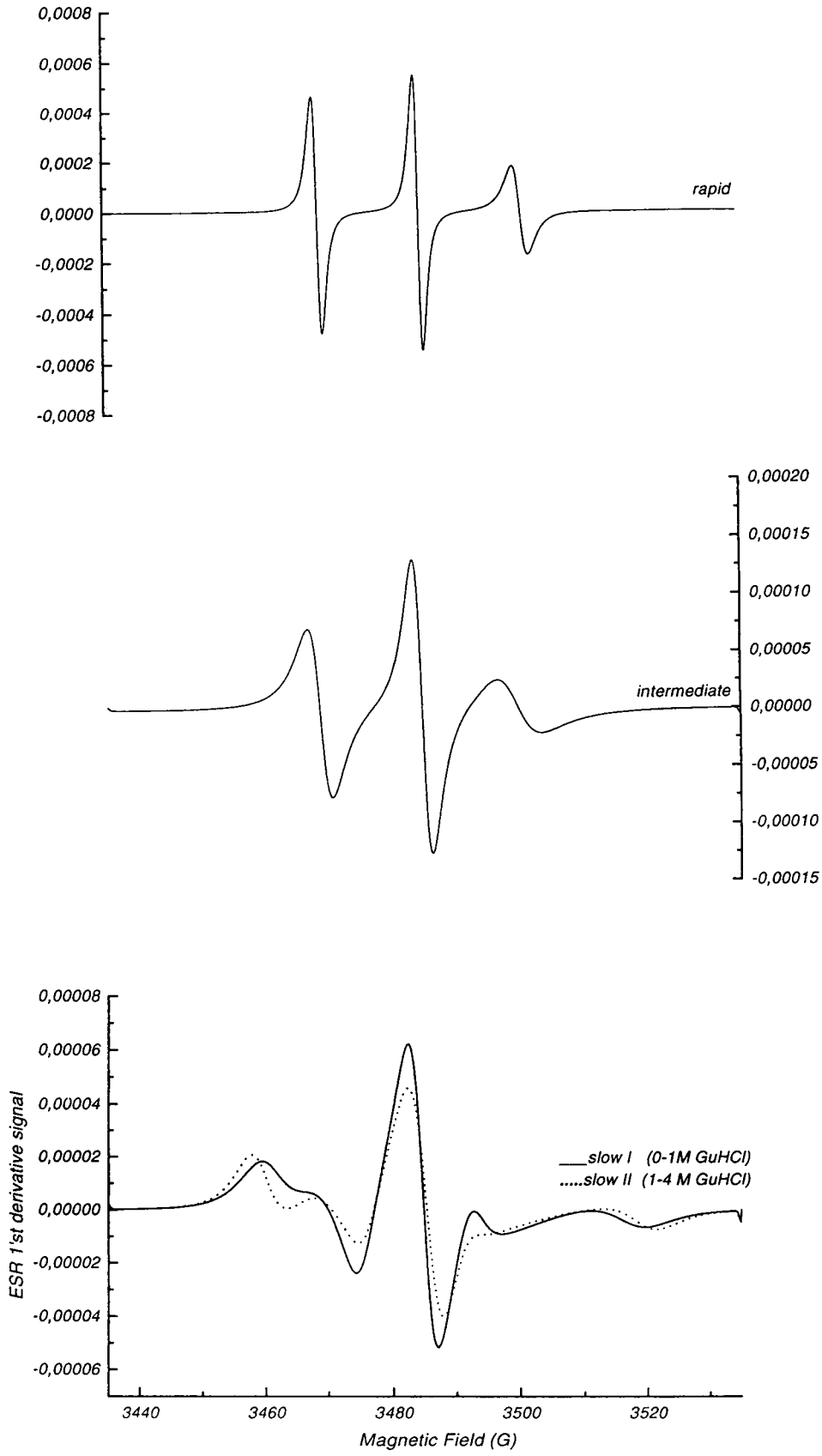

FIGURE 6 Simulations of the components of different mobility in spin-labeled cloned HCA II. Rapid: $d_{xy} = 0.22 \times 10^9\ s^{-1}$, $d_{zz} = 0.39 \times 10^9\ s^{-1}$, diffusion tilt = 75°, intrinsic line-width = 0.045 mT. Intermediate: $d_{xy} = 0.47 \times 10^8\ s^{-1}$, $d_{zz} = 1.4 \times 10^8\ s^{-1}$, diffusion tilt = 75°, intrinsic line-width = 0.023 mT. Slow I (below 1.1 M Gu-HCl): $d_{xy} = 0.20 \times 10^8\ s^{-1}$, $d_{zz} = 0.55 \times 10^8\ s^{-1}$, diffusion tilt = 30°, intrinsic line-width = 0.023 mT. Slow II (above 1.0 M Gu-HCl): $d_{xy} = 0.14 \times 10^8\ s^{-1}$, $d_{zz} = 0.14 \times 10^8\ s^{-1}$, intrinsic line-width = 0.075 mT. Hyperfine splitting and g-tensor components are given in Materials and Methods. The spectra were convoluted with a Gaussian function having the peak-to-peak line-width (first derivative) of 0.075 mT. This resulted in a line-width of 0.166 mT for the $m_I = 0$ transition of the most rapid component. 10G = 1 mT.

judged from the difference spectra obtained as explained in a previos section, an EPR signal associated with medium mobility should have a maximum at ~0.5–0.7 M Gu-HCl.

Starting with isotropic rotational diffusion parameters to account for the extrema separation, an appropriate fraction of the spectrum obtained was subtracted from the experimental spectra obtained at 0.5–0.7 M Gu-HCl to isolate a spectrum of the intermediate state. The same kind of information was obtained also by examining the difference spectra in which the slow and intermediate component dominated. The spectrum of the intermediate component was then simulated with an anisotropic diffusion model as it gave a better description of the relative amplitude and line-widths between the narrower center line and the broadened $m_I = +1$ and -1 transitions.

The procedure was then repeated in an iterative manner until a reasonable fit was obtained between the experimental spectrum obtained at 0 M and 0.5–0.7 M Gu-HCl, introducing an anisotropic diffusion model for the components of both slow and intermediate mobility.

The simulation of the rapid component was obtained by starting from the rotational diffusion parameters for the intermediate state and then increasing successively each of the d_{xy} and d_{zz} parameters until the relative amplitudes of the $m_I = -1$, 0, and $+1$, transitions, were satisfactorily reproduced. The parameters were chosen to fit the spectra obtained at 3.0 and 4.0 M Gu-HCl (essentially identical). The absolute amplitudes were then easily obtained by adjusting the intrinsic line-width parameter and making very minor readjustments of the rotational diffusion parameters.

As the Gaussian broadening parameter mainly reflects unresolved isotropic hyperfine interactions to hydrogens within the spin-label, this parameter was fixed to the same value throughout all simulated spectra. This means also that the procedure of simulating all superimposed spectra (as described below) was repeated and tested for various values of the Gaussian broadening parameter. Essentially the same quality of the fits could be established by choosing this parameter to be between 0.05 and ~0.1 mT. The spectra used in superpositions are depicted in Fig. 6. The associated dynamic and line-width parameters are given in the figure legend.

Superpositions of the rapid, intermediate, and slow components were used to fit experimental spectra with their individual weights obtained by using a standard least squares procedure. From the method employed (see experimental section) the weights along with its standard deviations could be estimated by assuming that the measurement error is simply the root mean square value of difference between the fitted and the experimental amplitude values (at each field datum). The result of such fitting is plotted in Fig. 8 where the experimental derivative spectra were used throughout. To more clearly show the contribution of the broad component the spectra of the synthetic absorption (integrated) signal is also shown along with simulations in Fig. 7.

Details of experimental conditions and relative weights used in superimposed spectra are shown in the figures and legends (Figs. 1 and 7).

During the course of the analysis it was noted that the simulation appropriate for the slow component at 0 M Gu-HCl did not fit in total width to the spectra obtained at higher concentrations of Gu-HCl. The physical origin of this phenomenon could possibly arise from a volume change associated with the folded structure and/or because the folded state is sensitive to viscosity changes in the Gu-HCl medium. Superimposed simulated spectra describing the experimental data above 1.1 M Gu-HCl were therefore fitted by using a slow component with modified parameters, see Fig. 6 (lower). As we currently are investigating a total number of six different double mutants of carbonic anhydrase with the spin-label introduced in various positions, we would like to return to this and related issues in forthcoming reports.

From the plot of the relative weights versus Gu-HCl concentration one observes several interesting features (Fig. 8). The most important findings are summarized as follows. First, there exists a protein population in which the spin-label is situated in a compact and rigid environment from 0 M Gu-HCl up to ~1.7–2.0 M Gu-HCl, well above the first transition in the optical absorption. Second, a protein population with the spin-label having an intermediate mobility is present at 0 M Gu-HCl (18 ± 2%). It increases in abundance to a maximum (~40%) at ~0.7 M and at higher Gu-HCl concentrations it gradually decreases. Third, a population with a flexible structure in the region around the spin-label appears at ~0.7–1.0 M Gu-HCl but does not become dominant until ~1.7–2.0 M Gu-HCl.

CONCLUDING REMARKS

The structure of HCA II is dominated by an extensive twisted β-structure formed by 10 β-strands that pass through the entire molecule, and the only cysteine residue, Cys206, in the protein is located at the edge of the 7th β-strand (Eriksson et al., 1988). This strand together with its neighboring strand (number 6) constitute the most hydrophobic parts of the enzyme (Bergenhem et al., 1989). The substructure, containing Cys206, forms a relatively thin wall between a hydrophobic part of the active site cavity and the outside surface of the molecule. Thus, we examined this substructure in HCA II during its denaturation by Gu-HCl by introducing a spin-probe at the cysteine in position 206 and followed the changes in the EPR line-shape occurring with increased concentration of the denaturant. With a differentiation technique, two distinct regions of changes were observed, i.e., at 0.7 and 2.0 M, the former associated with an increase of a spin-label fraction in an intermediate state of mobility and the latter with the increase of an even more mobile species. From a comparison of the transitions as detected by optical absorption data the component of intermediate mobility is likely to be associated with the

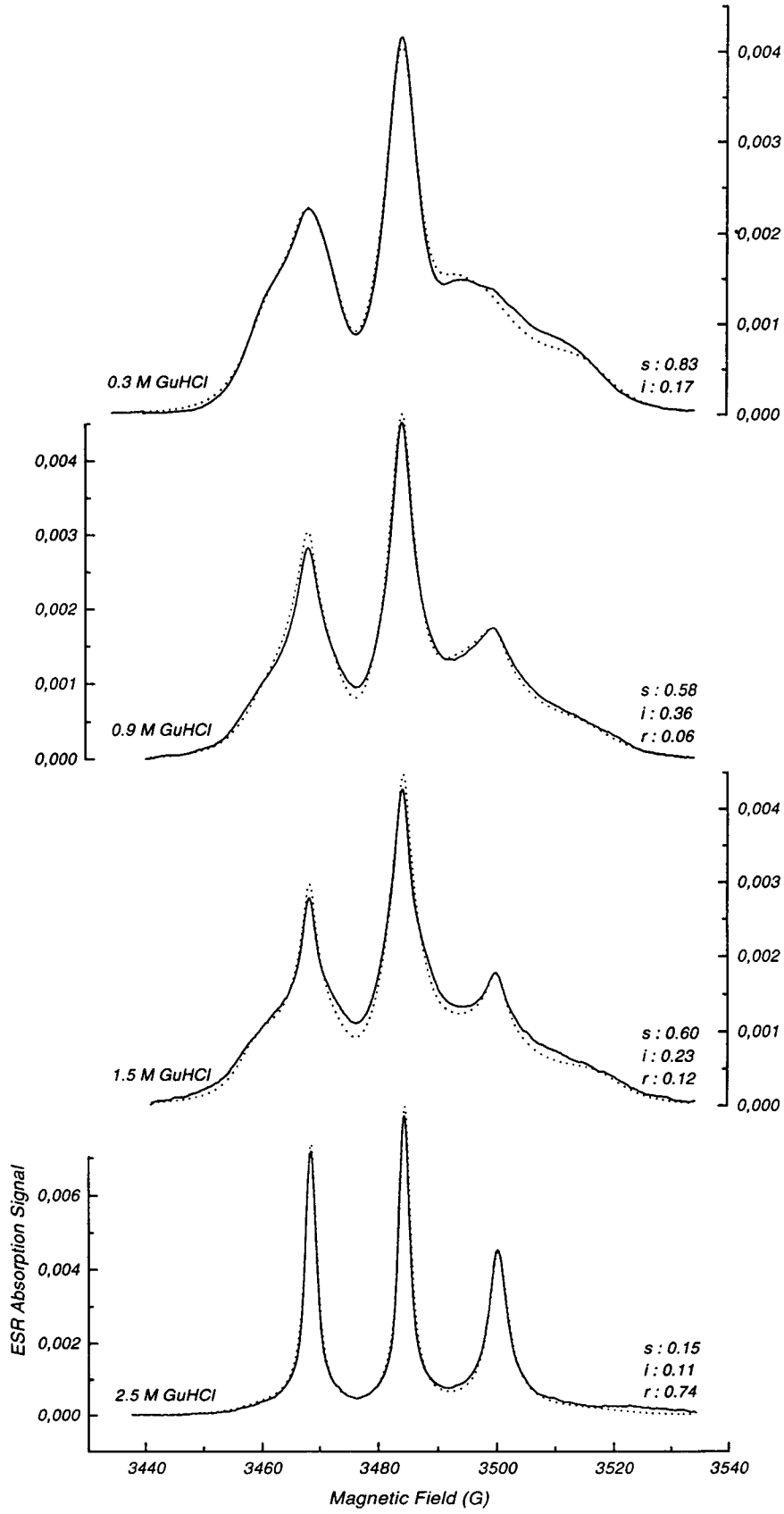

FIGURE 7 Absorption EPR spectra of cloned HCA II spin-labeled at the cysteine in position 206 recorded at selected denaturing agent (Gu-HCl) concentrations. The dashed curves are simulations produced as described in the text. The individual weight of the slow (s), intermediate (i), and rapid (r) component is given at each spectrum. All spectra are normalized and the scale beside each spectrum thus allows comparison of the amplitude at different Gu-HCl concentrations. 10G = 1 mT.

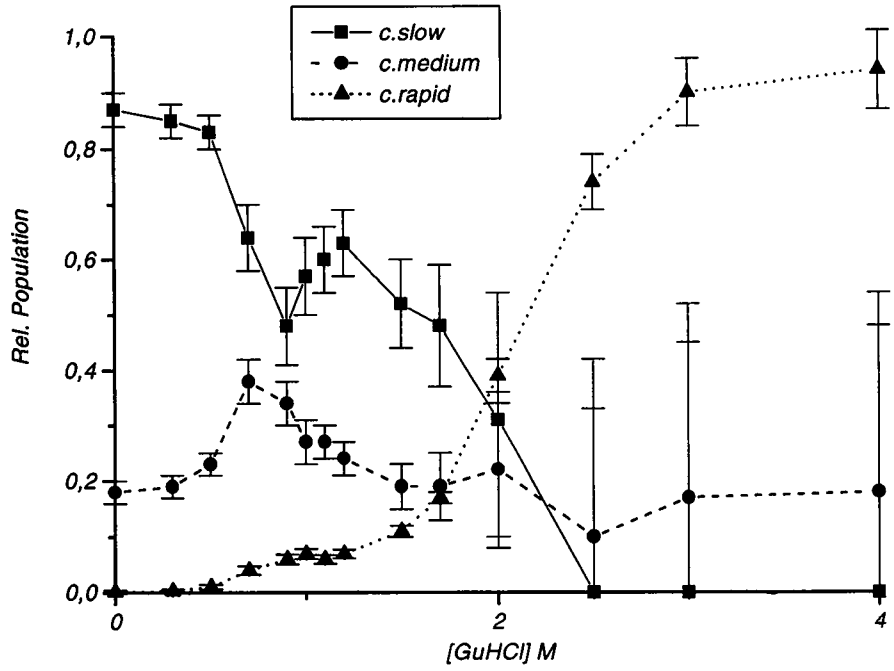

FIGURE 8 Relative abundances of slow, intermediate, and rapid component as obtained by least squares fitting to experimental data using superpositions of the simulations shown in Fig. 6. ■, slow component; ●, intermediate component; ▲, rapid component. Lines are drawn to guide the eye and have no other meaning. The error bar at each point represents the standard deviation of the fitted weight parameters. Further details are described in the text.

observed equilibrium folding intermediate. The EPR spectrum of the most mobile species is essentially the same as obtained at much higher Gu-HCl concentrations (3–5 M Gu-HCl) and thus cannot be distinguished from the unfolded state.

The rotational diffusion constants of each state of spin-label mobility were determined from line-shape simulations resulting in three distinct dynamic structures: slow, intermediate, and rapid. Interpreting these three dynamic structures as originating from three distinctly different protein conformations, the EPR results imply a complicated dynamic equilibrium between the folded, unfolded, and folding intermediate structures of carbonic anhydrase in the intermediate denaturation range (~0.5–2.0 M Gu-HCl). Our previous results, when monitoring the unfolding process at equilibrium by the change in A_{292}, have indicated the presence of a folding intermediate (at 1.0–2.0 M Gu-HCl). This parameter, A_{292}, can be considered to measure global changes of the protein structure. Other results, obtained for example from specific chemical labeling of various mutants of HCA II and fluorescence measurements on tryptophan mutants of the enzyme, have shown that this intermediate state has parts that are compact and other regions that are more fluctuating (Mårtensson et al., 1993, 1995; Svensson et al., 1995).

As the introduced spin-label is likely to probe structural changes and fluctuations in the local environment around position 206, the conclusions with regard to global protein structure must be taken with precaution. Possibly, the spin-label in the folding intermediate can have two main orientations: one toward a flexible part giving an intermediate diffusion constant and one orientation into a compact part. When the spin-label is situated in the compact part of the intermediate (molten-globule), its motion might be characterized by a diffusion constant very similar to that of the interior of the native protein. The appearance of the broad signals at Gu-HCl concentration between 1 and 2 M to a specific species can depend on such a situation; that is, the investigated substructure of the protein can form other compact states besides the native conformation.

The introduction of the EPR spectra differentiation technique shows a feasible way of detecting structural changes of a protein conformation. To obtain accurate results from such a procedure one has to record a series of EPR spectra at rather short intervals of a controllable experimental parameter (in our case, Gu-HCl concentration), shorter than the interval under which the changes one wants to study occur. Here it was shown that a plot of difference spectra amplitudes correlated very well with optical absorption data, suggesting that the effects detected by employing the two different experimental parameters in this case described the same (or at least related) phenomena. It was also shown how individual difference EPR spectra can guide in obtaining line-shape simulations of an intermediate state that otherwise would be quite difficult to obtain in a complicated superimposed spectrum. The simulations associated with the spin-probe in three different conformations could thereafter be used to fit the experimental spectra in a least squares sense throughout the whole concentration range, giving unique information concerning the local structure at the site of the spin-label and possibly also the populations of protein conformations, data that are not easily obtained by adopting other spectroscopic methods on HCA II and similar systems.

Altogether, the methods combined in this study appear to be a new way to obtain information of local conformational changes of proteins, and following this approach we are currently investigating the equilibrium folding intermediate

during the unfolding process in an extended series of spin-labeled HCA II mutants.

The following support is acknowledged: grants from the Swedish National Board for Technical Development (88–04392P to U.C. and B.-H.J.); the Swedish Natural Science Research Council (K-Ku 9426–300 to B.-H.J., K-Ku 4241–301 to U.C., and K7375–309 to M.L.); Stiftelsen Bengt Lundqvists Minne (M.S.); Sven och Lilly Lawskis Fond (P.-O.F. and L.-G.M.); Carl Trygger Foundation (M.L. and U.C.); and The Knut and Alice Wallenberg Foundation (M.L.).

REFERENCES

Altenbach, C., S. L. Flitsch, G. Khorana, W. L. Hubbell. 1989. Structural studies on transmembrane proteins. II. Spin labeling of bacteriorhodopsin mutants at unique cysteines. Biochemistry. 28:7806–7812.

Benetis, N. P., M. Lindgren, H.-S. Lee, A. Lund. 1990. Intramolecular dynamics in small radicals with anisotropic magnetic interactions. *Appl. Magn. Reson.* 1:267–278

Bergenhem, N., U. Carlsson, and J.-Å. Karlsson. 1989. Evidence for an initial fast nucleation process in the folding of human carbonic anhydrase I. *Int. J. Peptide Protein Res.* 33:140–145.

Calciano, L. J., W. A. Escobar, G. L. Millhausser, S. M. Miik, J. Rubaloff, A. P. Todd, and A. L. Fink. 1993. Side-chain mobility of the β-lactamase: a state probed by electron spin resonance spectroscopy. *Biochemistry.* 32:5644–5649.

Carlsson, U., R. Aasa, L. E. Henderson, B.-H. Jonsson, and S. Lindskog. 1975. Paramegnetic and fluorescent probes attached to "buried" sulfhydryl groups in human carbonic anhydrases: application to inhibitor binding, denaturation and refolding. *Eur. J. Biochem.* 52:25–36

Edsall, J. T., S. Mehta, D. V. Mayers, and J. M. Armstrong. 1966. Structure and denaturation of human carbonic anhydrases in urea and guanidine hydrochloride solutions. *Biochem. Z.* 345:9–36.

Endo, T. 1991. Control of protein function by antifolding and unfolding. *Kobunshi High Polymers Jpn.* 40:624–627.

Englander, S. W. 1993. In pursuit of protein folding. *Science.* 262: 848–849.

Eriksson, A. E., T. A. Jones, and A. Liljas. 1988. Refined structure of human carbonic anhydrase II at 2.0 Å resolution. *Proteins Struct. Funct. Genet.* 4:274–282.

Henkens, R. W., B. B. Kitchell, S. C. Lottich, P. J. Stein, and T. J. Williams. 1982. Detection and characterization using circular dichroism and fluorescence spectroscopy of a stable intermediate conformation formed in the denaturation of bovine carbonic anhydrase with guanidinium hydrochloride. *Biochemistry.* 21:5918–5923.

Khalifah, R. G., D. J. Strader, S. H. Bryant, and S. M. Gibson. 1977. Carbon C-13 nuclear magnetic resonance probe of active-site ionizations in human carbonic anhydrase B. *Biochemistry.* 16:2241–2247.

Lindgren, M., M. Svensson, P.-O. Freskgård, U. Carlsson, B.-H. Jonsson, L.-G. Mårtensson, and P. Jonasson. 1993. Probing local mobility in carbonic anhydrase: EPR of spin-labelled SH groups introduced by site-directed mutagenesis. *J. Chem. Soc. Perkin. Trans.* 2:2003–2007.

Mårtensson, L.-G., B.-H. Jonsson, M. Andersson, A. Kihlgren, N. Bergenhem, and U. Carlsson. 1992. Role of an evolutionarily invariant serine for the stability of human carbonic anhydrase II. *Biochim. Biophys. Acta.* 1118:179–186.

Mårtensson, L.-G., B.-H. Jonsson, P.-O. Freskgård, A. Kihlgren, M. Svensson, and U. Carlsson. 1993. Characterization of folding intermediates of human carbonic anhydrase II: probing substructure by chemical labeling of SH groups introduced by site-directed mutagenesis. *Biochemistry.* 32:224–231.

Mårtensson, L.-G., P. Jonasson, P.-O. Freskgård, M. Svensson, U. Carlsson, and B.-H. Jonsson. 1995. Contribution of individual tryptophan residues to the fluorescence spectrum of native and denatured forms of human carbonic anhydrase II. *Biochemistry.* 34:1011–1021.

Millhausser, G. L. 1992. Selective placement of electron spin resonance spin labels: new structural methods for peptides and proteins. *Trends Biochem. Sci.* 17:448–452.

Nair, S. K., T. L. Calderone, D. W. Christianson, and C. A. Fierke. 1991. Altering the mouth of a hydrophobic pocket: structure and kinetics of human carbonic anhydrase II mutants at residue Val-121. *J. Biol. Chem.* 266:17320–17325.

Pain, R. 1987. Protein folding for pleasure and for profit. *Trends Biochem. Sci.* 12:309–312.

Poole, C. P. Jr., H. A. Farach. 1986. Theory of Magnetic Resonance. John Wiley & Sons, New York.

Press, W. H., B. P. Flannery, S. A. Teukolsky, W. T. Wetterling. 1989. Numerical Recipes (FORTRAN Version). Cambridge University Press, Cambridge.

Schneider, D. J., and J. H. Freed. 1989. Calculating slow motional magnetic resonance spectra: a user's guide. *In* Biological Magnetic Resonance, Vol. 8: Spin Labeling Theory and Applications. L. J. Berliner and J. Reuben, editors. Plenum Press, New York. 1–76.

Shin, Y.-K., C. Levinthal, F. Levinthal, W. L. Hubbel. 1993. Colicin E1 binding to membranes: time-resolved studies of spin-labeled mutants. *Science.* 259:960–963.

Svensson, M., P. Jonasson, P.-O. Freskgård, B.-H. Jonsson, M. Lindgren, L.-G. Mårtensson, M. Gentile, K. Borén, and U. Carlsson. 1995. Mapping the folding intermediate of human carbonic anhydrase II. Probing substructure by chemical reactivity and spin- and fluorescent labeling of engineered cysteine residues. *Biochemistry.* In press.

Todd, A. P., J. Cong, F. Levinthal, C. Levinthal, W. L. Hubbel. 1989. Site-directed mutagenesis of colicin E1 provides specific attachment sites for spin labels whose spectra are sensitive to local conformation. *Proteins Struct. Funct. Genet.* 6:294–305.